[CANCER RESEARCH 63, 4568–4576, August 1, 2003]

FUS/ERG Gene Fusions in Ewing's Tumors

Danielle C. Shing, Dominic J. McMullan, Paul Roberts, Kim Smith, Suet-Feung Chin, James Nicholson, Roger M. Tillman, Pramila Ramani, Catherine Cullinane, and Nicholas Coleman[1]

Medical Research Council Cancer Cell Unit, Hutchison/MRC Research Centre, Cambridge, CB2 2XZ [D. C. S., N. C.]; West Midlands Regional Cytogenetics Laboratory, Birmingham Women's Hospital, Birmingham, B15 2TG [D. J. M.]; Departments of Cytogenetics [P. R.] and Pathology [C. C.], St. James's University Hospital, Leeds, LS9 7TF; Cytogenetics, Department of Medical Genetics [K. S.] and Department of Paediatric Oncology [J. N.], Addenbrooke's NHS Trust, Cambridge, CB2 2QQ; University of Cambridge/Cancer Research United Kingdom Department of Oncology, Cambridge, CB2 2XZ [S-F. C.]; The Royal Orthopaedic Hospital NHS Trust, Bristol Road South, Birmingham, B31 2AP [R. M. T.]; and Department of Pathology, Birmingham Children's Hospital, Birmingham, B4 6NH [P. R.], United Kingdom

ABSTRACT

Ewing's tumors are rare pediatric neoplasms that are characterized by specific chromosomal translocations and gene rearrangements. All of the fusion genes reported to date in Ewing's tumors juxtapose the *EWS* gene at 22q12 to an *ETS*-related gene, the most common of which are *FLI1* at 11q24 and *ERG* at 21q22. We present here four cases of Ewing's tumor, which showed no evidence of a *EWS* gene rearrangement, but instead contained translocations involving 16p11 and 21q22. A rearrangement involving the same chromosome bands, t(16;21)(p11;q22), is found in rare cases of acute myeloid leukemia and fuses the *FUS* gene at 16p11 to the *ERG* gene at 21q22. In two of our Ewing's tumor cases, we were able to show at the sequence level that the translocation between chromosomes 16 and 21 similarly results in a *FUS/ERG* fusion. In one case, exons 1–5 and most of exon 6 of *FUS* were fused in-frame to exon 9 of *ERG*; in the other case, *FUS* exons 1–7 were fused in-frame to *ERG* exons 8–9. The functional fusion transcript is expected to be expressed from the der(21)t(16;21) derivative. In the two other t(16;21)-positive Ewing's cases, we performed bacterial artificial chromosome fluorescence *in situ* hybridization analysis on metaphases and interphase nuclei to demonstrate colocalization of bacterial artificial chromosomes containing *FUS* and *ERG* genes, also highly suggestive of fusion gene formation. These represent the first four cases where *FUS*, rather than *EWS*, is rearranged with an *ETS*-family transcription factor in Ewing's tumors. Our data provide additional evidence that the transactivation domains of the TET family of RNA-binding proteins (such as EWS and FUS) are interchangeable, and suggests a novel mechanism of oncogenesis in Ewing's tumors.

INTRODUCTION

Ewing's tumors are rare pediatric neoplasms that include Ewing's sarcoma, Askin's tumor, and peripheral primitive neuroectodermal tumors (1). Ewing's tumors are characterized cytogenetically by rearrangements of the *EWS* gene at 22q12 with members of the *ETS* family of transcription factors. In 85% of cases, *EWS* is fused with *FLI1* at 11q24 (2, 3). In analogous rearrangements, *EWS* is fused to *ERG* at 21q22 in 5–10% of Ewing's tumors (4), and to *ETV1* at 7p22 (5), *E1AF* at 17q12 (6, 7), or *FEV* at 2q33 (8) in <1% of cases. The resultant fusion genes are thought to encode aberrant transcription factors that are composed of the NH_2-terminal transactivation domain of EWS and the COOH-terminal DNA-binding domain of the ETS-related gene. It is presumed that an altered pattern of gene expression results and that this is of importance in neoplastic transformation (9).

EWS is a member of the TET family of RNA-binding proteins, which also includes FUS (TLS; Refs. 10, 11) and $TAF_{II}68$ (RBP56 or TAF2N; Refs. 12, 13). TET proteins have similar genomic structures, are ubiquitously expressed (14, 15), and are believed to act as adaptors between transcription and RNA processing, a function that involves their COOH-terminal RNA-binding domains (12, 16). Interestingly, FUS −/− mice have suggested an important role for FUS in genomic maintenance and stability (17, 18).

The NH_2-terminal domains of TET proteins are potent transactivators (16, 19–22) that are juxtaposed to the DNA-binding domains of transcription factors in a number of mesenchymal proliferations (10, 11, 23–32), as well as in some cases of AML[2] and acute lymphoid leukemia (33–36). The transcription factor partners include ETS-family proteins, but also a range of other molecules. As with the COOH-terminal DNA-binding domains of ETS-related proteins, the NH_2-terminal transactivation domains of TET family proteins appear to be functionally interchangeable, both *in vitro* (16) and *in vivo*. For example, myxoid liposarcoma can arise either from a *FUS/CHOP* (10, 11) or a *EWS/CHOP* fusion (27), extraskeletal myxoid chondrosarcoma can result from either a *EWS/CHN* (25, 26) or a $TAF_{II}68/CHN$ fusion (28, 31, 32), and acute leukemia from a *EWS/CIZ* or a $TAF_{II}68/CIZ$ fusion (36). In general, it is the transcription factor component of the fusion protein that specifies the tumor type. As an example, fusion of an *ETS*-related gene to *EWS* appears to be specific for Ewing's tumors. However, there are exceptions, because the ETS transcription factor, ERG, can contribute its DNA-binding domain both to EWS in Ewing's tumors and also to FUS in t(16;21)(p11;q22)-positive AMLs (33–35). Similarly, the *ATF1* gene is fused to *EWS* in clear cell sarcoma (23) and to *FUS* in angiomatoid fibrous histiocytoma (30).

All of the fusion genes reported to date in Ewing's tumors have involved the NH_2 terminus of EWS and the COOH terminus of an ETS family member. In this paper, we describe four Ewing's tumors that were not rearranged at 22q12 and instead possessed a novel primary translocation t(16;21)(p11;q22), cytogenetically identical to that found in rare cases of AML. In all of the four cases, we have demonstrated the formation of a *FUS/ERG* fusion gene. These represent the first reported cases of Ewing's tumors where the primary translocation involved a rearrangement of the *FUS* gene, rather than *EWS*, suggesting a novel mechanism of oncogenesis in Ewing's tumors.

MATERIALS AND METHODS

Case Reports

We studied four cases of Ewing's tumor, named ET-1, ET-2, ET-3, and ET-4. Details of the clinicopathological features of these cases are given in Table 1, and representative histological and immunohistochemical images are shown in Fig. 1. In all of the cases, the histopathological diagnosis of Ewing's tumor was made by a consultant histopathologist. All of the cases were reviewed subsequently by at least two other consultant histopathologists and confirmed as showing the features of Ewing's tumor. In particular, the possibility that the tumors studied represented solid deposits of AML was definitively excluded in each case. Bone marrow biopsies and/or aspirates were

Received 3/3/03; accepted 5/22/03.

The costs of publication of this article were defrayed in part by the payment of page charges. This article must therefore be hereby marked *advertisement* in accordance with 18 U.S.C. Section 1734 solely to indicate this fact.

[1] To whom requests for reprints should be addressed, at Medical Research Council Cancer Cell Unit, Hutchison/MRC Research Centre, Hills Road, Cambridge CB2 2XZ, United Kingdom. Phone: 44-1223-763285; Fax: 44-1223-763284; E-mail: nc109@cam.ac.uk.

[2] The abbreviations used are: AML, acute myeloid leukemia; BAC, bacterial artificial chromosome; CGH, comparative genomic hybridization; FISH, fluorescence *in situ* hybridization; gDNA, genomic DNA; M-FISH, multiplex-fluorescence *in situ* hybridization; PBL, peripheral blood lymphocyte; RT-PCR, reverse transcription-PCR; SKY, spectral karyotyping.

Table 1 *Clinicopathologic details for the four Ewing's tumour cases studied*

Case	ET-1	ET-2	ET-3	ET-4
Age/sex	9/M	7/F	15/F	21/M
Clinical presentation	Firm, ill-defined lump beneath right nipple.	Chest wall mass.	Right-sided chest and back pain and tiredness.	Pain and swelling in left thigh.
Site of primary tumor	Chest wall	Chest wall	Chest wall	Left femur
Histology	Malignant tumor composed of islands of small round blue cells with frequent mitotic activity.	Malignant tumor composed of sheets of small round blue cells with frequent mitotic activity.	Malignant tumor composed of nests of closely packed small round cells showing moderate pleomorphism, numerous mitoses and focal necrosis.	Periosteum and bone infiltrated by a malignant round cell tumour showing focal necrosis.
Immunophenotype	Expression of vimentin, neural markers and surface CD99. No expression of myogenic, lymphoid or myeloid markers.	Weak, patchy expression of surface CD99; no expression of neural, myogenic, lymphoid or myeloid markers.	Expression of surface CD99; no expression of neural, myogenic, lymphoid or myeloid markers.	Expression of surface CD99 and focal expression of muscle-specific actin; no expression of other myogenic markers, nor of neural, lymphoid or myeloid markers.
Diagnosis	Askin's tumour	Askin's tumour	Askin's tumour	Ewing's sarcoma
Clinical outcome	Died 2 years after diagnosis.	Alive	Alive	Alive

performed on each patient and showed no evidence of AML or other hematological malignancy.

In case ET-1, samples were available from an initial biopsy (ET-1a) and from a subsequent resection (ET-1b). With the exception of ET-1b, all of the samples were obtained before any chemotherapy or radiotherapy.

Cytogenetics

Conventional Cytogenetic Analysis. Cells were short-term cultured and metaphases prepared according to standard protocols (37, 38). Karyotyping was carried out using conventional cytogenetic G banding.

Molecular Cytogenetics. Metaphases were available from ET-1a and ET-2 for additional karyotyping by molecular cytogenetic techniques. We undertook 24-color painting and SKY analysis of tumor metaphases using protocols that we have described elsewhere (39, 40). We subsequently designed four-color and seven-color "tailored" paint sets for M-FISH to confirm and refine the abnormalities detected by SKY (39, 40).

CGH. gDNA was extracted from snap-frozen tissue from ET-1a using proteinase K and phenol:chloroform extraction. CGH was carried out as described previously (40, 41) using normal PBL gDNA as a reference. On the basis of normal:normal hybridizations, thresholds were set at 0.85 for loss and 1.15 for gain.

BAC-FISH. BAC DNA was extracted using an alkaline lysis protocol from the following BAC clones: 222M10, containing the *EWS* gene (42); 428J4, containing *FLI1* (42); RP11–388M20, containing *FUS* (Wellcome Trust Sanger Institute, Hinxton, Cambridgeshire, United Kingdom); RP11–476D17, containing the 3′ end of the *ERG* gene; and RP11–95I21, containing the 5′ end of the *ERG* gene (both from BACPAC Resources, Children's Hospital Oakland Research Institute, Oakland, CA).

BAC DNA was labeled by nick translation (Vysis, Richmond, United Kingdom) with SpectrumOrange-dUTP (Vysis), biotin-16-dUTP, or digoxigenin-11-dUTP (Roche, Lewes, United Kingdom). Whole chromosome paints were made and labeled by degenerate oligonucleotide primed PCR, as described previously (39, 40).

Labeled BACs and whole chromosome paints were ethanol coprecipitated with a 50-fold excess (w/w) of Cot-1 DNA (Roche) and hybridized onto tumor metaphase chromosomes using standard protocols (39). Immunofluorescent detection of biotin and digoxigenin labels was performed using avidin-Cy5 (Amersham Biosciences, Little Chalfont, United Kingdom) and antidigoxigenin FITC-conjugated Fab fragments (Roche), respectively (39, 40). Images were visualized on an epifluorescence microscope (Zeiss, Welwyn Garden City, United Kingdom) using SmartCapture VP imaging software (Digital Scientific, Cambridge, United Kingdom).

Interphase FISH. Interphase FISH was performed using a three-color BAC probe set consisting of BAC clones RP11–388M20 (containing *FUS*) labeled with SpectrumOrange, RP11–476D17 (containing 3′ end of *ERG* gene) labeled with digoxigenin, and RP11–95I21 (containing 5′ end of *ERG* gene) labeled with biotin. Interphase FISH was carried out on a fixed cell suspension prepared from short-term cultures of case ET-4, using a standard FISH protocol (39, 40) and on paraffin-embedded tissue sections of case ET-3 using the following method.

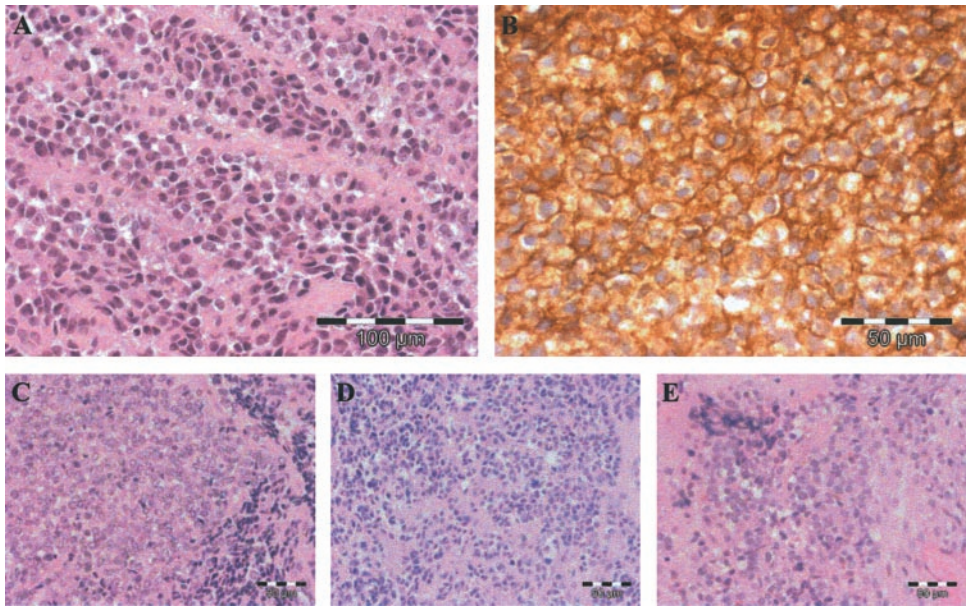

Fig. 1. Representative histological and immunohistochemical images of the four Ewing's tumor cases studied. *A* and *B*, Case ET-1 stained with H&E (*A*) and by immunohistochemistry for CD99 (*B*). *C–E*, cases ET-2, ET-3, and ET-4, respectively, all stained by H&E. All four tumors showed the typical histopathological features of Ewing's tumors, being composed of islands and nests of "small round blue cells" showing an appropriate immunohistochemical profile, including cell surface expression of CD99 (Table 1). There was no morphological evidence of myeloid differentiation and no evidence of expression of myeloid markers by histochemistry and immunohistochemistry. The possibility that the tumors represented solid deposits of AML was definitively excluded in each case.

Paraffin-embedded tissue sections (5 μm) were cut onto slides coated with 3-aminopropyl-triethoxysilane (Sigma, Poole, United Kingdom). Slides were dewaxed by immersion in xylene for 10 min at room temperature three times, then dehydrated in 70%, 90%, and 100% ethanol for 5 min each before being air-dried. Slides were pretreated by incubation in 0.01 M citric acid (pH 6.0) at 80°C for 2 h and were then washed twice in 2× SSC. Tissue was digested using 10 mg/ml pepsin in 0.2 M HCl (pH 2.0) at 37°C for 15 min. Slides were washed in 2× SSC, dehydrated through a series of 70%, 90%, and 100% ethanol, and air-dried.

Probe containing labeled BACs was applied to each slide, overlaid with a coverslip, and sealed with rubber gum. The slides and probes were codenatured at 80°C for 10 min and allowed to hybridize in a humidified chamber at 37°C for 3 days. Immunofluorescence detection of the indirect labels biotin and digoxigenin was carried out using avidin-Cy5 and antidigoxigenin FITC-conjugated Fab fragments, respectively, as described previously (39, 40), with the additional step of ethanol dehydration before 4′,6-diamidino-2-phenylindole counterstaining. Images were captured on an epifluorescence microscope using SmartCapture VP imaging software, as described for BAC-FISH.

Molecular Genetic Analysis

RT-PCR for Detection of Fusion Transcripts. mRNA was extracted from snap-frozen tissue of ET-1a, ET-1b, and ET-4 using a Quickprep Micro mRNA Purification kit (Amersham Biosciences). The mRNA was treated with RQ1 RNase-Free DNase (Promega, Madison, WI) and reverse transcribed to cDNA using a Reverse Transcription System (Promega). RT-PCR was carried out for *EWS/FLI1* using primers EWS 22.3 and FLI1 11.3 (3); for *EWS/ERG* using primers EWS22.8 and ERG11 (4, 43); and for *FUS/ERG* using primers TLS0F (27) and ERG11 (43), followed by a 1:25 dilution of PCR products, and nested PCR using primers TLS35F (27) and ERG12 (Table 2). An annealing temperature of 60°C was used for all of the reactions. The RT-PCR products were run on a 1% agarose gel, and *FUS/ERG* products were extracted for sequencing using a QIAquick Gel Extraction kit (Qiagen, Crawley, United Kingdom).

Mapping of gDNA Breakpoints by Long-Range PCR and Chromosome Walking. Long-range PCR for the genomic *FUS/ERG* fusion gene was performed on gDNA from ET-1a and ET-1b using TLS0F and ERG11 primers and an Expand Long Template PCR System (Roche). PCR cycling conditions were as recommended by the manufacturer, and an annealing temperature of 60°C was used. To refine the analysis of the breakpoint, primers were designed in *FUS* exon 6, and in *ERG* intron 8 and *ERG* exon 9 (Table 2). The long-range PCR product was diluted 1:10 and amplified using the TLSex6–1 forward primer, and reverse primers in ERG intron 8 and ERG exon 9. An annealing temperature of 56°C was used in these reactions. PCR products were run on a 1% agarose gel, and the product from TLSex6–1 and ERGin8–1 primers was extracted using a QIAquick Gel Extraction kit for sequencing.

Sequencing. Sequencing of gel-purified PCR products was carried out in both forward and reverse directions using a DYEnamic ET Terminator Cycle Sequencing kit (Amersham Biosciences) according to the manufacturer's instructions. Sequencing products were run on an ABI 3100 sequencer (Applied Biosystems, Foster City, CA).

RESULTS

Conventional Cytogenetic Analysis of Four Ewing's t(16;21) Cases

A United Kingdom Children's Cancer Study Group study of Ewing's tumors revealed four cases, named ET-1, ET-2, ET-3, and ET-4, carrying translocations that juxtaposed chromosome bands 16p11 and 21q22, instead of a classical t(11;22)(q24;q12) or variant chromosome 22 rearrangement. The primary translocation seen in ET-1 was t(16;21;22)(p11;q22;p11.2); in ET-2 was t(16;21)(p11.2;q22.3); in ET-3 was a der(21)t(16;21)(p11;q22); and in ET-4 was t(16;21)(p11;q22). In all four of the cases, a derivative chromosome, der(21)t(16;21)(p11;q22), was present.

A t(16;21)(p11;q22) translocation in AML results in the formation of a *FUS/ERG* fusion gene, transcribed from the derivative chromosome 21 (33–35). Therefore, we wished to test whether *FUS* and *ERG* can be rearranged in Ewing's tumors. We were able to carry out detailed molecular genetic analysis on two of our cases, ET-1 and ET-4, as well as BAC-FISH analysis on the other two cases.

Case ET-1

Molecular Cytogenetic Analysis. SKY analysis and subsequent four-color and seven-color M-FISH analysis of ET-1a confirmed the karyotype seen by conventional cytogenetics (Fig. 2, *A* and *B;* data not shown). A three-way translocation, t(16;21;22)(p11;q22;p11.2; Fig. 2*C*) was the only structural rearrangement present. Numerical abnormalities included gains of chromosomes 5, 8, and 12, confirmed by CGH (Fig. 2*D*). Only a limited number of metaphases was available, and we were therefore unable to perform BAC-FISH using BACs containing the *EWS*, *FLI1*, *FUS*, and *ERG* genes.

Evidence for a *FUS/ERG* Transcript by RT-PCR. *EWS/FLI1* and *EWS/ERG* fusion transcripts were not detected in ET-1a and ET-1b by RT-PCR (data not shown). However, nested RT-PCR for the *FUS/ERG* fusion transcript in ET-1a, using outer primers TLS0F and ERG11, and inner primers TLS35F and ERG12 (Fig. 3*A*), gave a product of 875 bp (Fig. 3*B*). This product was not present in the Ewing's cell line, LAP-35, which is known to contain a classical t(11;22)(q24;q12) translocation and to express the *EWS/FLI1* fusion transcript (40).

Table 2 *Primers used in PCR reactions*

The locations of primers in FUS (TLS) and ERG are shown in Fig. 3A.

Gene	Primer	Exon/intron	Direction	Sequence 5′-3′	Reference
EWS	EWS22.8	Exon 7	Forward	ccc act agt tac cca ccc caa a	(4)
	EWS22.3	Exon 7	Forward	tcc tac agc caa gct cca agt c	(3)
FUS	TLS0F	Exon 1	Forward	cgt cgg tgc tca gcg gtg ttg	(27)
	TLS35F	Exon 1	Forward	gcg cgg aca tgg cct caa acg	(27)
	TLSex6-1	Exon 6	Forward	tgg cgg tta tgg caa tca ag	—
FLI1	FLI1 11.3	Exon 9	Reverse	act ccc cgt tgg tcc cct cc	(3)
ERG	ERGin8-1	Intron 8	Reverse	caa att cca gtt aca gca ctg cct	—
	ERGin8-2	Intron 8	Reverse	gtt tat ggc tcc cta gaa gac agc a	—
	ERGin8-3	Intron 8	Reverse	tcc cct tgg gaa gct gaa tg	—
	ERGin8-4	Intron 8	Reverse	cct tgc ctg tgt gct gca ac	—
	ERGin8-5	Intron 8	Reverse	ttg ctg gcg ctc aga aag c	—
	ERGin8-6	Intron 8	Reverse	gtg gat ggc aat aat gac tta atg c	—
	ERGin8-7	Intron 8	Reverse	ggg caa agt tca ggc tgc ttc	—
	ERGin8-8	Intron 8	Reverse	gtt cca ggg gaa aga ggc tct c	—
	ERGex9-1	Exon 9	Reverse	cca gga gga act gcc aaa gc	—
	ERG12	Exon 9	Reverse	cgg gat ccg tca tct tga act c	—
	ERG11	Exon 9	Reverse	tgt tgg gtt tgc tct tcc gct c	(43)
	ERGex9-2	Exon 9	Reverse	cga tcc cgt gga agt cga ac	—
GAPDH	GAPDH F	Exon 7	Forward	aca gtc cat gcc atc act gcc	—
	GAPDH R	Exon 7	Reverse	gcc tgc ttc acc acc ttc ttg	—

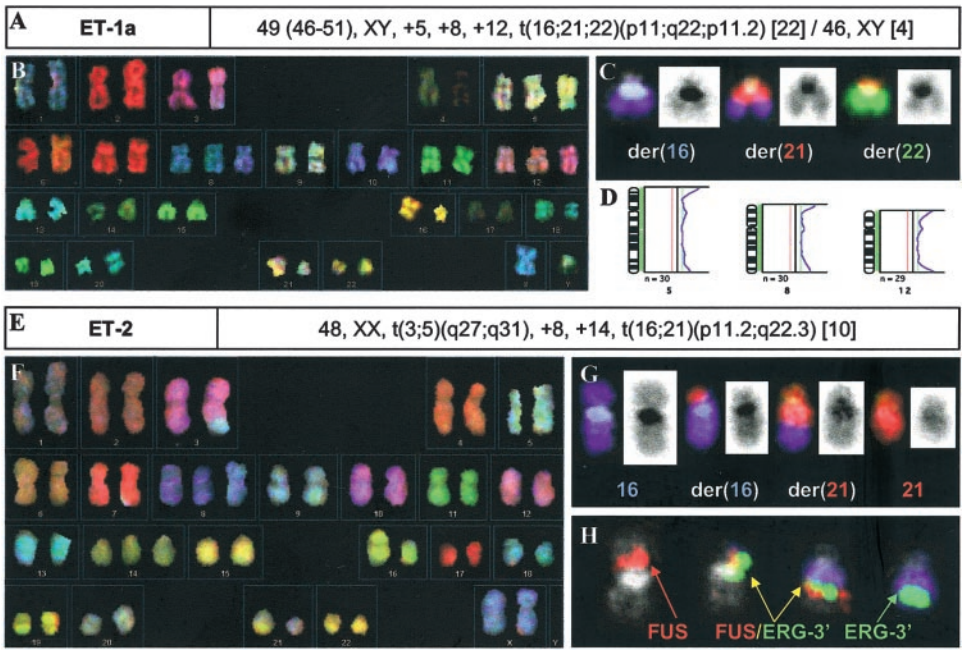

Fig. 2. Molecular cytogenetic analysis of ET-1a and ET-2. *A*, karyotype of ET-1a, as determined by conventional cytogenetics and confirmed by molecular cytogenetics. *B*, 24-color painting of ET-1a, depicted in SKY display colors. *C*, detailed view of derivative chromosomes 16, 21, and 22 of t(16;21;22)(p11;q22;p11.2) in ET-1a, after four-color tailored M-FISH. Chromosome 16 is painted *blue*, chromosome 21 *red*, and chromosome 22 *green*. *D*, CGH in ET-1a demonstrates gain of chromosomes 5, 8, and 12. *E*, karyotype of ET-2, as determined by conventional cytogenetics and confirmed by molecular cytogenetics. *F*, 24-color painting of ET-2, depicted in SKY display colors. *G*, detailed view of t(16;21)(p11.2;q22.3) balanced translocation in ET-2, following four-color tailored M-FISH. Chromosome 16 is painted *blue* and chromosome 21 *red*. *H*, BAC-FISH analysis of t(16;21)(p11.2;q22.3) in ET-B2. BACs containing *FUS* (RP11–388M20, *red*) and the 3′ end of the *ERG* gene (RP11–476D17, *green*) give split and colocalized signals on the derivative chromosomes 16 and 21, der(16) and der(21). Chromosome 16 is *unpainted* and chromosome 21 is *blue*.

Sequence of the *FUS/ERG* Transcript. The *FUS/ERG* RT-PCR product from ET-1a was sequenced and revealed a transcript that consisted of *FUS* exons 1–6 (except the last 10 nucleotides of exon 6) at the 5′ end, fused in-frame with the whole of *ERG* exon 9 at the 3′ end. The sequence of the *FUS/ERG* cDNA breakpoint is shown in Fig. 3*C*.

Mapping of the gDNA *FUS/ERG* Breakpoint. gDNA of ET-1a and ET-1b was amplified by long-range PCR using the same primers as for RT-PCR, TLS0F in *FUS* exon 1 and ERG11 in *ERG* exon 9 (Fig. 3*A*). A genomic *FUS/ERG* product of 7–8 kb was seen in both specimens (Fig. 3*E*). We deduced that ~5 kb of this product was represented by *FUS* exons 1–6, inclusive of intronic sequences, because the *FUS* breakpoint had been shown by RT-PCR to lie within exon 6. We concluded that the genomic breakpoint of *ERG* would lie in *ERG* intron 8, approximately 2–3 kb 5′ to *ERG* exon 9.

To refine the analysis of the genomic breakpoint, a forward primer (TLSex6–1) was designed in *FUS* exon 6, and a series of reverse primers were designed spanning 2 kb in *ERG* intron 8 and *ERG* exon 9 (Fig. 3*A*). The long-range PCR product of ET-1a (Fig. 3*E*) was diluted and amplified with the TLSex6–1 forward primer and the series of *ERG* reverse primers (Fig. 3, *A* and *F*). Sequencing of the smallest product, from primers TLSex6–1 and ERGin8–1, identified that the rearrangement occurred at a TGG trinucleotide sequence shared between *FUS* exon 6 (located 7–9 nucleotides from the 3′ end of the exon) and *ERG* intron 8 (located 2096–2098 nucleotides from the 3′ end of *ERG* exon 9; Fig. 4, *A* and *B*). The fusion created a new splice site within *FUS* exon 6. Therefore, the last 10 nucleotides of *FUS* exon 6 were absent from the fusion transcript (Fig. 4*C*).

As both the *FUS* gene on 16p and the *ERG* gene on 21q lie telomeric to centromeric, we deduce that the functional *FUS/ERG* fusion gene would be expressed from the der(21)t(16;21)(p11;q22) derivative chromosome.

Case ET-2

Molecular Cytogenetic Analysis. Molecular cytogenetic analysis of ET-2, by SKY (Fig. 2*F*) and tailored seven-color and four-color M-FISH (data not shown) confirmed the abnormalities detected by conventional cytogenetics (Fig. 2*E*). A balanced translocation t(16;21)(p11.2;q22.3) was present (Fig. 2*G*), and the der(21)t(16;21) appeared cytogenetically identical to that in case ET-1 (Fig. 2*C*). Other abnormalities included a reciprocal t(3;5)(q27;q31) translocation, trisomy 8 and trisomy 14.

BAC-FISH on metaphase chromosomes confirmed the absence of a *EWS/FLI1* fusion gene (data not shown). BACs containing the *FUS* gene and the 3′ end of the *ERG* gene gave split signals on the der(16) and der(21) derivative chromosomes of the t(16;21)(p11.2;q22.3) translocation, suggesting that the genomic breakpoints were contained within these BACs (Fig. 2*H*). Colocalization of the BACs containing *FUS* and the 3′ DNA-binding domain of *ERG* strongly suggests that a *FUS/ERG* fusion gene was present in ET-2.

Case ET-3

Interphase FISH Analysis. Conventional cytogenetic analysis of ET-3 revealed one normal chromosome 16, one normal chromosome 21, and a der(21)t(16;21)(p11;q22) derivative (Fig. 5*B*). Metaphases were not available for molecular cytogenetics. Therefore, we designed a three-color BAC probe set to test for rearrangements of *FUS* and *ERG* by interphase FISH analysis of paraffin-embedded tissue sections of ET-3. BACs containing *FUS* were labeled in red, those containing the 3′ end of *ERG* in green, and those containing the 5′ end of *ERG* in blue. This combination would produce a red-green fusion signal if *FUS* was juxtaposed to the 3′ end of the *ERG* gene. A red-green-blue signal would be seen if 16p11 and 21q22 colocalized by chance [a der(16)t(16;21) being absent in this case]. We analyzed 120 tumor nuclei and 120 normal nuclei from different regions of the same tissue section. Consistent with the karyotype of ET-3, a single red signal, representing chromosome 16, was observed in 66% of tumor nuclei, and a single green-blue signal, representing chromosome 21, in 68% of tumor nuclei. Red-green-blue signals were observed in 3% of tumor and 9% of normal nuclei. A red-green signal, representing the der(21)t(16;21), was observed in 75% of tumor nuclei and in only 1% of normal nuclei (χ^2 test, $P < 0.001$; Fig. 5*B*), strongly suggesting that a *FUS/ERG* fusion gene was present in this case.

Case ET-4

Interphase FISH Analysis. Conventional cytogenetic analysis of ET-4 revealed that the tumor contained both derivatives of a t(16;

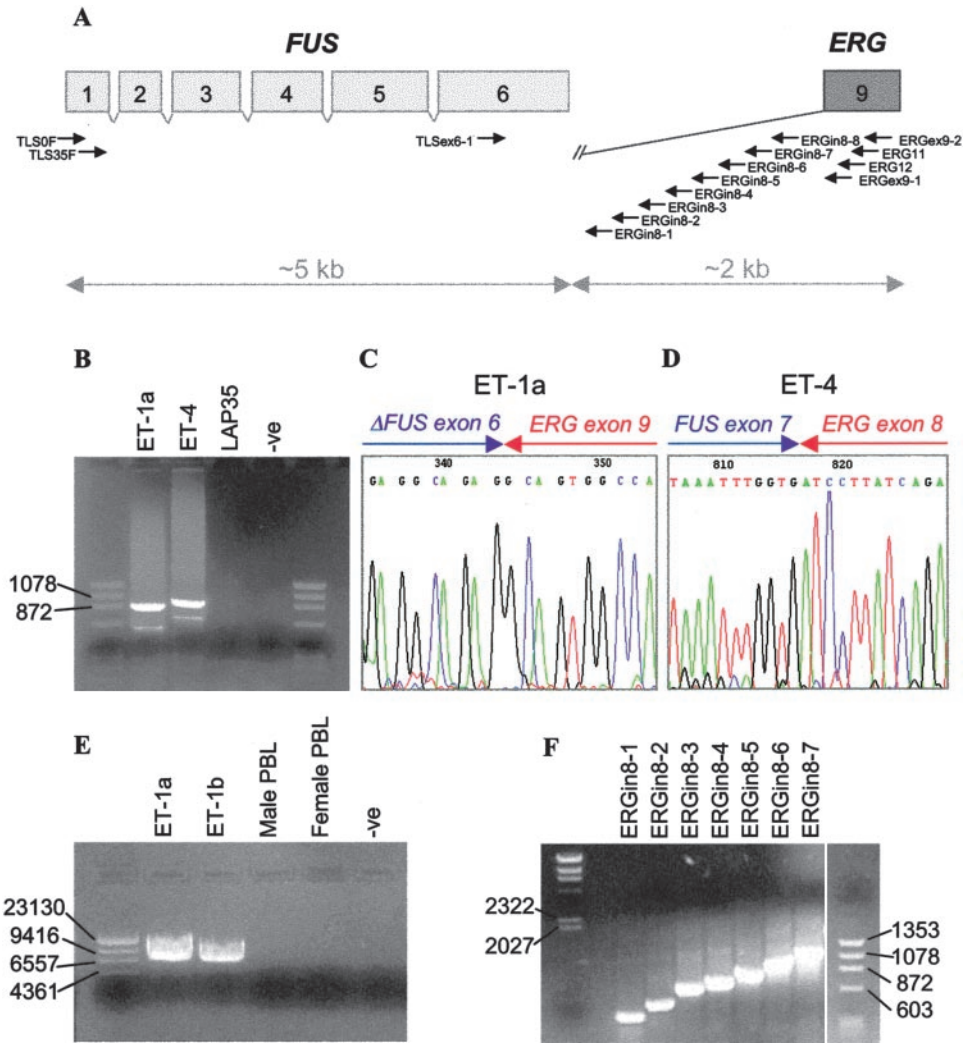

Fig. 3. Evidence of *FUS/ERG* fusion transcript in ET-1a and ET-4 by RT-PCR (*A–D*) and mapping of genomic *FUS/ERG* breakpoint in ET-1 by long-range PCR and chromosome walking (*A*, *E*, and *F*). *A*, location of primers in *FUS* exons 1–6 and *ERG* intron 8 and exon 9 used to map *FUS/ERG* breakpoint in cDNA and gDNA. *B*, nested RT-PCR for *FUS/ERG* on three samples. A fusion transcript is detectable in ET-1a and ET-4, but not in LAP35, a Ewing's tumor cell line that expresses *EWS/FLI1*. *C*, sequence of the *FUS/ERG* transcript breakpoint in ET-1a. *FUS* exons 1–5 and most of exon 6 are fused in-frame to *ERG* exon 9 (see also Fig. 4). *D*, sequence of the *FUS/ERG* transcript breakpoint in ET-4. *FUS* exons 1–7 are fused in-frame to *ERG* exons 8–9. *E*, long-range PCR on ET-1a and ET-1b gDNA using TLS0F and ERG11 primers. A *FUS/ERG* fusion product of 7–8 kb is present in ET-1, but absent in normal male and female PBLs. *F*, chromosome walking along the genomic *FUS/ERG* fusion in ET-1a. Long-range genomic *FUS/ERG* PCR product from ET-1a (*E*) was diluted 1:10 and amplified using TLSex6–1 forward primer and reverse primers shown in *A*.

21)(p11;q22) translocation, two normal copies of chromosome 16, and one normal copy of chromosome 21 (Fig. 5*C*). Metaphases were not available for molecular cytogenetics. Interphase FISH analysis of 100 tumor nuclei was performed on a fixed cell suspension of ET-4, using a three-color BAC probe set (*FUS* in red, *ERG-3′* in green, and *ERG-5′* in blue). Two single red signals, representing the two normal copies of chromosome 16, were observed in 64% of nuclei and one green-blue signal, representing the normal chromosome 21, was pres-

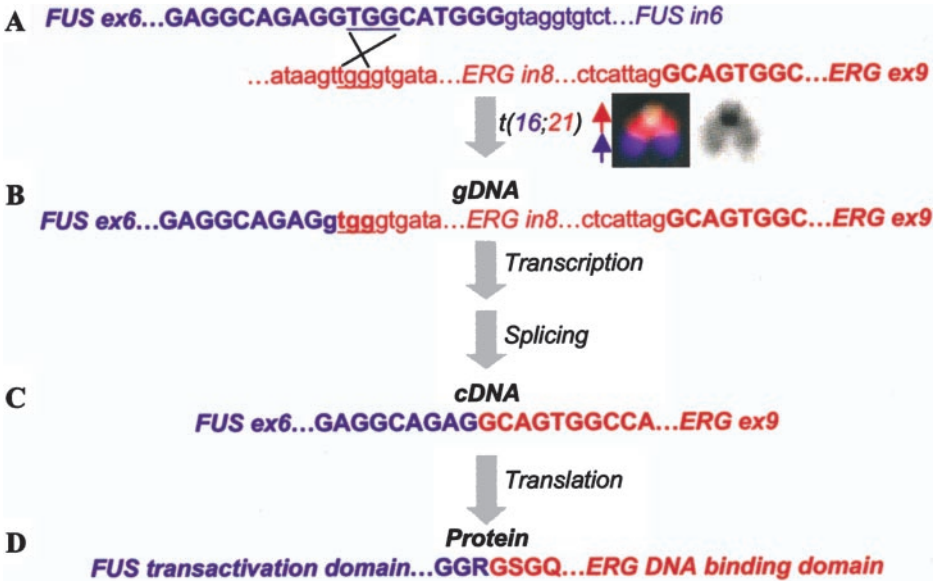

Fig. 4. Schematic to show rearrangement of *FUS* and *ERG* genes in ET-1. *A*, *FUS* and *ERG* genomic sequences at 16p11 and 21q22, respectively, before rearrangement. A trinucleotide sequence, TGG, is shared between *FUS* exon 6 and *ERG* intron 8. *ex*, exon; *in*, intron; *uppercase*, exon sequence; *lowercase*, intron sequence. *B*, translocation between chromosomes 16 and 21 gives rise to a *FUS/ERG* fusion gene. The genomic sequence of the der(21), from which *FUS/ERG* is expressed, is shown. Fusion of *FUS* exon 6 to *ERG* intron 8 creates a new splice site. *C*, transcription and splicing of *FUS/ERG* gives rise to an in-frame fusion transcript, composed of exons 1–5 plus a truncated exon 6 of *FUS* and exon 9 of *ERG*. *D*, translation is presumed to produce a *FUS/ERG* fusion protein.

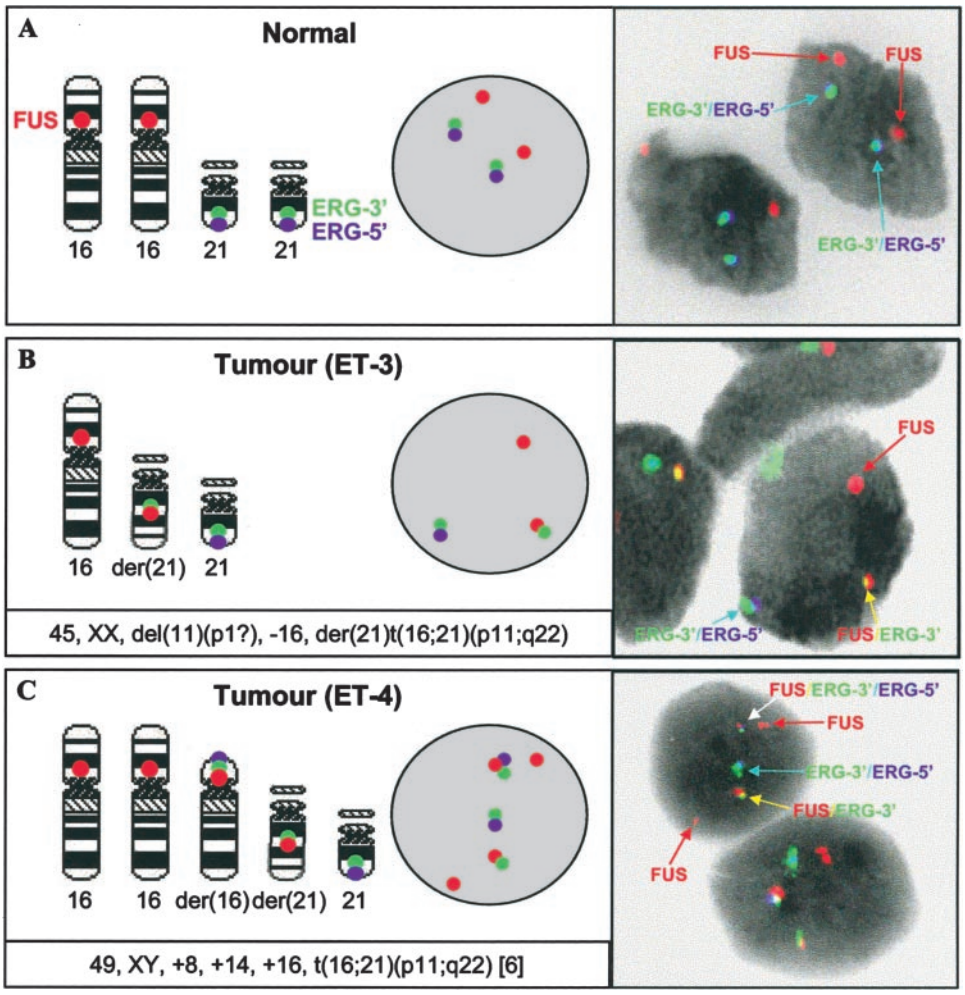

Fig. 5. Interphase FISH analysis of ET-3 and ET-4. On the basis of the karyotypes of ET-3 and ET-4, the signals that would be predicted if a *FUS/ERG* fusion was present are shown on the *left* of each panel. *A*, interphase FISH on normal nuclei from ET-3, using BACs containing the *FUS* gene (RP11–388M20, *red*), the 3′ end of the *ERG* gene (RP11–476D17, *green*) and the 5′ end of the *ERG* gene (RP11–95I21, *blue*). *B*, interphase FISH on tumor nuclei from ET-3, using the BACs described above. Note that the der(16)t(16;21) has been lost in this tumor. A red-green *FUS/ERG-3′* fusion signal was observed in 75% of tumor nuclei. *C*, interphase FISH on tumor nuclei from ET-4, using the BACs described above. A red-green *FUS/ERG-3′* fusion signal, representing the der(21)t(16;21), was observed in 82% of tumor nuclei, whereas a red-green-blue *FUS/ERG-3′/ERG-5′* fusion signal (producing *white* in the *lower nucleus*), representing the der(16)t(16;21), was seen in 71% of tumor nuclei.

ent in 76% of nuclei. A red-green signal, representing the *FUS/ERG* fusion gene on the der(21)t(16;21), was observed in 82% of nuclei, and a red-green-blue signal, representing the reciprocal *ERG/FUS* gene on the der(16)t(16;21), was observed in 71% of nuclei. The high proportion of cells containing *FUS/ERG* and *ERG/FUS* fusion signals strongly suggests that these genes were rearranged in ET-4.

Evidence for a *FUS/ERG* Transcript by RT-PCR and Sequencing. Nested RT-PCR for the *FUS/ERG* transcript in ET-4, using outer primers TLS0F and ERG11 and inner primers TLS35F and ERG12, gave a product of size 969 bp (Fig. 3*B*). Sequencing revealed that the transcript consisted of *FUS* exons 1–7 and *ERG* exons 8–9 (Fig. 3*D*), suggesting that the genomic breakpoints were within *FUS* intron 7 and *ERG* intron 7.

DISCUSSION

All of the cases of Ewing's tumor reported to date have involved rearrangement of the *EWS* gene, at 22q12, with an ETS-family transcription factor. Here we present four Ewing's tumor cases in which there are primary rearrangements that juxtapose chromosome bands 16p11 and 21q22, abnormalities that have not been reported previously in Ewing's tumors. Detailed genetic analysis of two of these cases, ET-1 and ET-4, has revealed that this rearrangement results in the fusion of the *FUS* gene at 16p11 to the *ERG* gene at 21q22. In the other two cases, ET-2 and ET-3, BAC-FISH on metaphase chromosomes and interphase nuclei, respectively, strongly suggests that these cases also possess a *FUS/ERG* fusion gene, with the breakpoint in *ERG* lying toward the 3′ end of the gene.

For the two cases where sequence data were available, ET-1 and ET-4, a *FUS/ERG* fusion gene was formed on the der(21)t(16;21), and an in-frame fusion transcript was expressed. In ET-1, the transcript consisted of *FUS* exons 1–5, most of exon 6, and *ERG* exon 9, whereas in ET-4, the transcript was composed of *FUS* exons 1–7 and *ERG* exons 8–9. In both cases, the translated fusion proteins would comprise the transactivation domain of FUS and the DNA-binding domain of the ETS-family transcription factor ERG, thus resembling the more common Ewing's tumor fusion proteins EWS/FLI1 and EWS/ERG. These represent the first Ewing's tumor cases where the primary chromosomal rearrangement involves the *FUS* gene and not *EWS*.

Although formation of a *FUS/ERG* fusion gene has not been described previously in Ewing's tumors, it is known to be a rare but recurrent primary event in AML (34, 35). The presence of t(16;21)(p11;q22) in AML is associated with a younger age at presentation, the median age at diagnosis being 22 in t(16;21)- positive AML cases, but >60 in all cases of AML combined (44). Because t(16;21)(p11;q22) has only been observed to date in the four Ewing's tumor cases described here, it is not yet known whether the presence of this translocation could be clinically significant. Interestingly, three of the cases that we describe were Askin's tumors of the chest wall. However, the overall prevalence of the *FUS/ERG* fusion gene in Ewing's tumors *in vivo* is not known.

We observed that the *FUS/ERG* genomic breakpoint of case ET-1 occurred at a TGG sequence that was shared between the *FUS* and *ERG* genes. This trinucleotide sequence is present frequently at translocation junctions of similar fusion genes, such as *FUS/CHOP* and *EWS/CHOP* in myxoid liposarcoma and *FUS/ERG* in AML (45).

It is not clear how a rearrangement between the same two genes can give rise to a leukemia (AML) in one instance and a sarcoma (Ewing's tumor) in another. It is possible that *FUS/ERG* activates the same oncogenic mechanism in both neoplasms, and it is the cell lineage in which the translocation occurs that determines the tumor type. Alternatively, *FUS/ERG* may activate different oncogenic pathways in AML and in Ewing's tumor, as different numbers of exons make up the fusion gene in each case. In an individual AML patient, there is expression either of three alternatively spliced transcripts, types A-C, or of a single transcript, type D (Fig. 6*A*; Refs. 35, 44). Only types B and D are in-frame. Type B *FUS/ERG* transcripts fuse *FUS* exons 1–7 to *ERG* exon 9, whereas type D transcripts fuse *FUS* exons 1–8 and *ERG* exons 7–9. Whole exons are involved, as the genomic breakpoints in AML are within intronic sequences (44, 45). In the two Ewing's tumor cases presented here for which sequence data are available, novel fusion gene structures are observed, which we have named types E and F (Fig. 6*A*). Exon 9 of *ERG* is always included in *FUS/ERG* fusion genes, because it encodes the DNA-binding domain of the transcription factor.

The variation in the *FUS* breakpoints between the *FUS/ERG* of AML and the *FUS/ERG* of our Ewing's tumor cases (Fig. 6*A*) may be of significance in terms of the effect on the domain structures of the EWS and FUS proteins (Fig. 6*B*). The NH_2-terminal transactivation domains of EWS and FUS can be subdivided into two independent functional domains TR1 and TR2 (Fig. 6*B*; Ref. 46). TR1 comprises exons 1–5 of *FUS* and exons 1–7 of *EWS*, whereas TR2 is made up of exons 6–7 of *FUS* and exons 8–9 of *EWS*. Deletion studies on the FUS/ERG fusion protein have shown that whereas TR1 is necessary for transformation of mouse fibroblast NIH3T3 cells, TR2 is essential for transformation of a mouse myeloid precursor cell line L-G, suggesting that the TR2 domain has leukemogenic potential (46). The two domains may also activate independent oncogenic pathways. Therefore, it may be of importance that *FUS* exons 1–7 (representing TR1 and TR2 domains) are always included in AML *FUS/ERG* transcripts, whereas the TR2 domain appears to be dispensable in solid tumors. In the most common Ewing's tumor fusion transcripts *EWS/FLI1* and *EWS/ERG*, only *EWS* exons 1–7 (TR1 domain only) are involved (46). Although the TR2 domain (*FUS* exons 6–7) is intact in our Ewing's tumor case ET-4, it would be disrupted in case ET-1, because

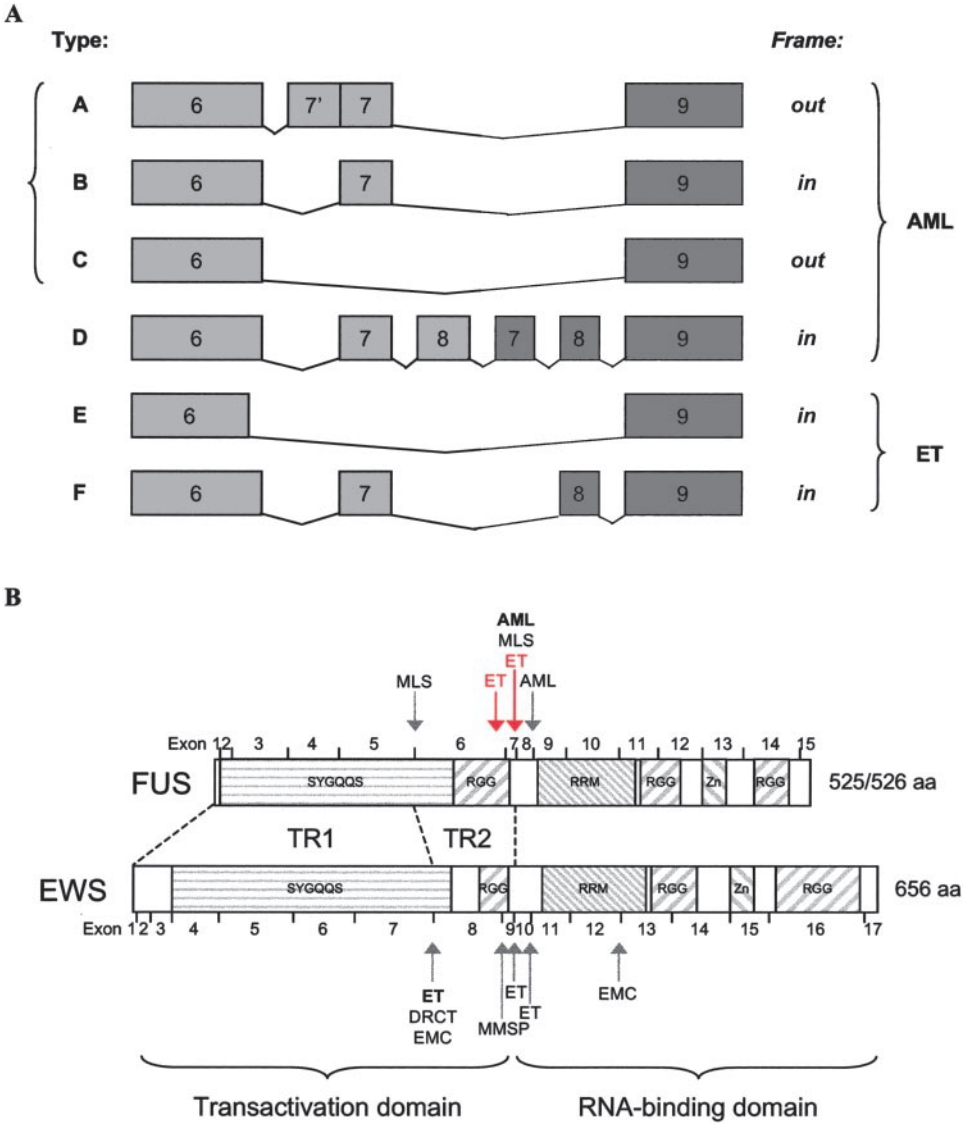

Fig. 6. Comparison of the *FUS/ERG* exon structures seen in AML with those in the Ewing's tumors ET-1 and ET-4 (*A*) and domain structures of FUS and EWS proteins (*B*). *A*, in AML, there is expression either of three transcripts, types *A–C*, of which only type *B* is in-frame, or of one transcript, type *D* (44). The *FUS/ERG* transcript types labeled *E* and *F* were observed in Ewing's tumor cases ET-1 and ET-4, respectively. *B*, homologous domains of the TET proteins FUS and EWS include *SYGQQS*, degenerative Ser-Tyr-Gly-Gln-Gln-Ser repeats; *RGG*, Arg-Gly-Gly triplet-rich repeat region; *RRM*, RNA-recognition motif; and *Zn*, zinc finger motif. *Arrows* indicate FUS and EWS breakpoints in myxoid liposarcoma (*MLS*), AML, Ewing's tumor (*ET*), desmoplastic small round cell tumor (*DRCT*), extraskeletal myxoid chondrosarcoma (*EMC*), and malignant melanoma of soft parts (*MMSP*). Where the breakpoint in a given tumor is variable, the most common breakpoint is shown in *bold*. The *red arrows* indicate the FUS breakpoints in our Ewing's tumor cases ET-1 and ET-4.

the breakpoint of *FUS* lies within exon 6. Absence of this leukemogenic domain might favor an oncogenic pathway distinct from the one activated in AML.

Although it is unusual for a primary translocation and fusion gene to be shared between a soft tissue proliferation and a leukemia or lymphoma, there are two additional examples in the literature. A t(12;15)(p13;q25) translocation with resultant *ETV6/NTKR3* fusion gene has been reported in both congenital fibrosarcoma (47) and a single case of AML (Ref. 48; as well as secretory breast carcinoma; Ref. 49), whereas a t(1;2)(q25;p23) translocation and *TPM3/ALK* fusion gene can lead to either inflammatory myofibroblastic tumor (50) or anaplastic large cell lymphoma (51, 52). In both of these examples, the fusion proteins act as constitutively active tyrosine kinases (53). To our knowledge, FUS/ERG represents the first case of an aberrant transcription factor shared between a sarcoma and a leukemia/lymphoma.

In summary, the four Ewing's tumor cases presented in this study may represent a novel class of Ewing's tumor in which 22q12 is not rearranged, and instead the primary translocation involves chromosomes 16 and 21. Demonstration, in all four of the cases, two by sequencing and two by BAC-FISH, that the t(16;21)(p11;q22) translocation gives rise to a *FUS/ERG* fusion gene suggests a novel mechanism of oncogenesis in Ewing's tumors, where the transactivation domain of FUS, rather than that of EWS, contributes to aberrant gene expression and transformation. Fusion of *FUS* with other ETS-family genes may also occur in Ewing's tumors. Interestingly, *FUS/FLI1* fusions have not been reported, despite *FLI1* being the most common fusion partner for *EWS* in Ewing's tumors. Therefore, it is possible that *ERG* is the preferred ETS-family fusion partner for *FUS*. The precise clinical significance of the alternative mechanism of Ewing's tumor formation that we have described remains to be determined.

REFERENCES

1. Sandberg, A. A., and Bridge, J. A. Updates on cytogenetics and molecular genetics of bone and soft tissue tumors: Ewing sarcoma and peripheral primitive neuroectodermal tumors. Cancer Genet. Cytogenet., *123:* 1–26, 2000.
2. Turc-Carel, C., Aurias, A., Mugneret, F., Lizard, S., Sidaner, I., Volk, C., Thiery, J. P., Olschwang, S., Philip, I., Berger, M. P., Philip, T., Lenoir, G. M., and Mazabraud, A. Chromosomes in Ewing's sarcoma. I. An evaluation of 85 cases of remarkable consistency of t(11;22)(q24;q12). Cancer Genet. Cytogenet., *32:* 229–238, 1988.
3. Delattre, O., Zucman, J., Plougastel, B., Desmaze, C., Melot, T., Peter, M., Kovar, H., Joubert, I., de Jong, P., and Rouleau, G. Gene fusion with an ETS DNA-binding domain caused by chromosome translocation in human tumours. Nature (Lond.), *359:* 162–165, 1992.
4. Zucman, J., Melot, T., Desmaze, C., Ghysdael, J., Plougastel, B., Peter, M., Zucker, J. M., Triche, T. J., Sheer, D., Turc-Carel, C., Ambros, P., Combaret, V., Lenoir, G., Aurias, A., Thomas, G., and Delattre, O. Combinatorial generation of variable fusion proteins in the Ewing family of tumours. EMBO J., *12:* 4481–4487, 1993.
5. Jeon, I. S., Davis, J. N., Braun, B. S., Sublett, J. E., Roussel, M. F., Denny, C. T., and Shapiro, D. N. A variant Ewing's sarcoma translocation (7;22) fuses the EWS gene to the ETS gene ETV1. Oncogene, *10:* 1229–1234, 1995.
6. Kaneko, Y., Yoshida, K., Handa, M., Toyoda, Y., Nishihira, H., Tanaka, Y., Sasaki, Y., Ishida, S., Higashino, F., and Fujinaga, K. Fusion of an ETS-family gene, EIAF, to EWS by t(17;22)(q12;q12) chromosome translocation in an undifferentiated sarcoma of infancy. Genes Chromosomes Cancer, *15:* 115–121, 1996.
7. Urano, F., Umezawa, A., Hong, W., Kikuchi, H., and Hata, J. A novel chimera gene between EWS and E1A-F, encoding the adenovirus E1A enhancer-binding protein, in extraosseous Ewing's sarcoma. Biochem. Biophys. Res. Commun., *219:* 608–612, 1996.
8. Peter, M., Couturier, J., Pacquement, H., Michon, J., Thomas, G., Magdelenat, H., and Delattre, O. A new member of the ETS family fused to EWS in Ewing tumors. Oncogene, *14:* 1159–1164, 1997.
9. Arvand, A., and Denny, C. T. Biology of EWS/ETS fusions in Ewing's family tumors. Oncogene, *20:* 5747–5754, 2001.
10. Crozat, A., Aman, P., Mandahl, N., and Ron, D. Fusion of CHOP to a novel RNA-binding protein in human myxoid liposarcoma. Nature (Lond.), *363:* 640–644, 1993.
11. Rabbitts, T. H., Forster, A., Larson, R., and Nathan, P. Fusion of the dominant negative transcription regulator CHOP with a novel gene FUS by translocation t(12;16) in malignant liposarcoma. Nat. Genet., *4:* 175–180, 1993.
12. Bertolotti, A., Lutz, Y., Heard, D. J., Chambon, P., and Tora, L. hTAF(II)68, a novel RNA/ssDNA-binding protein with homology to the pro-oncoproteins TLS/FUS and EWS is associated with both TFIID and RNA polymerase II. EMBO J., *15:* 5022–5031, 1996.
13. Morohoshi, F., Arai, K., Takahashi, E. I., Tanigami, A., and Ohki, M. Cloning and mapping of a human RBP56 gene encoding a putative RNA binding protein similar to FUS/TLS and EWS proteins. Genomics, *38:* 51–57, 1996.
14. Morohoshi, F., Ootsuka, Y., Arai, K., Ichikawa, H., Mitani, S., Munakata, N., and Ohki, M. Genomic structure of the human RBP56/hTAFII68 and FUS/TLS genes. Gene, *221:* 191–198, 1998.
15. Aman, P., Panagopoulos, I., Lassen, C., Fioretos, T., Mencinger, M., Toresson, H., Hoglund, M., Forster, A., Rabbitts, T. H., Ron, D., Mandahl, N., and Mitelman, F. Expression patterns of the human sarcoma-associated genes FUS and EWS and the genomic structure of FUS. Genomics, *37:* 1–8, 1996.
16. Zinszner, H., Albalat, R., and Ron, D. A novel effector domain from the RNA-binding protein TLS or EWS is required for oncogenic transformation by CHOP. Genes Dev., *8:* 2513–2526, 1994.
17. Kuroda, M., Sok, J., Webb, L., Baechtold, H., Urano, F., Yin, Y., Chung, P., de Rooij, D. G., Akhmedov, A., Ashley, T., and Ron, D. Male sterility and enhanced radiation sensitivity in TLS(−/−) mice. EMBO J., *19:* 453–462, 2000.
18. Hicks, G. G., Singh, N., Nashabi, A., Mai, S., Bozek, G., Klewes, L., Arapovic, D., White, E. K., Koury, M. J., Oltz, E. M., Van Kaer, L., and Ruley, H. E. Fus deficiency in mice results in defective B-lymphocyte development and activation, high levels of chromosomal instability and perinatal death. Nat. Genet., *24:* 175–179, 2000.
19. Bertolotti, A., Bell, B., and Tora, L. The N-terminal domain of human TAFII68 displays transactivation and oncogenic properties. Oncogene, *18:* 8000–8010, 1999.
20. Prasad, D. D., Ouchida, M., Lee, L., Rao, V. N., and Reddy, E. S. TLS/FUS fusion domain of TLS/FUS-erg chimeric protein resulting from the t(16;21) chromosomal translocation in human myeloid leukemia functions as a transcriptional activation domain. Oncogene, *9:* 3717–3729, 1994.
21. May, W. A., Gishizky, M. L., Lessnick, S. L., Lunsford, L. B., Lewis, B. C., Delattre, O., Zucman, J., Thomas, G., and Denny, C. T. Ewing sarcoma 11;22 translocation produces a chimeric transcription factor that requires the DNA-binding domain encoded by FLI1 for transformation. Proc. Natl. Acad. Sci. USA, *90:* 5752–5756, 1993.
22. May, W. A., Lessnick, S. L., Braun, B. S., Klemsz, M., Lewis, B. C., Lunsford, L. B., Hromas, R., and Denny, C. T. The Ewing's sarcoma EWS/FLI-1 fusion gene encodes a more potent transcriptional activator and is a more powerful transforming gene than FLI-1. Mol. Cell. Biol., *13:* 7393–7398, 1993.
23. Zucman, J., Delattre, O., Desmaze, C., Epstein, A. L., Stenman, G., Speleman, F., Fletchers, C. D., Aurias, A., and Thomas, G. EWS and ATF-1 gene fusion induced by t(12;22) translocation in malignant melanoma of soft parts. Nat. Genet., *4:* 341–345, 1993.
24. Ladanyi, M., and Gerald, W. Fusion of the EWS and WT1 genes in the desmoplastic small round cell tumor. Cancer Res., *54:* 2837–2840, 1994.
25. Clark, J., Benjamin, H., Gill, S., Sidhar, S., Goodwin, G., Crew, J., Gusterson, B. A., Shipley, J., and Cooper, C. S. Fusion of the EWS gene to CHN, a member of the steroid/thyroid receptor gene superfamily, in a human myxoid chondrosarcoma. Oncogene, *12:* 229–235, 1996.
26. Brody, R. I., Ueda, T., Hamelin, A., Jhanwar, S. C., Bridge, J. A., Healey, J. H., Huvos, A. G., Gerald, W. L., and Ladanyi, M. Molecular analysis of the fusion of EWS to an orphan nuclear receptor gene in extraskeletal myxoid chondrosarcoma. Am. J. Pathol., *150:* 1049–1058, 1997.
27. Panagopoulos, I., Hoglund, M., Mertens, F., Mandahl, N., Mitelman, F., and Aman, P. Fusion of the EWS and CHOP genes in myxoid liposarcoma. Oncogene, *12:* 489–494, 1996.
28. Panagopoulos, I., Mencinger, M., Dietrich, C. U., Bjerkehagen, B., Saeter, G., Mertens, F., Mandahl, N., and Heim, S. Fusion of the RBP56 and CHN genes in extraskeletal myxoid chondrosarcomas with translocation t(9;17)(q22;q11). Oncogene, *18:* 7594–7598, 1999.
29. Mastrangelo, T., Modena, P., Tornielli, S., Bullrich, F., Testi, M. A., Mezzelani, A., Radice, P., Azzarelli, A., Pilotti, S., Croce, C. M., Pierotti, M. A., and Sozzi, G. A novel zinc finger gene is fused to EWS in small round cell tumor. Oncogene, *19:* 3799–3804, 2000.
30. Waters, B. L., Panagopoulos, I., and Allen, E. F. Genetic characterization of angiomatoid fibrous histiocytoma identifies fusion of the FUS and ATF-1 genes induced by a chromosomal translocation involving bands 12q13 and 16p11. Cancer Genet. Cytogenet., *121:* 109–116, 2000.
31. Attwooll, C., Tariq, M., Harris, M., Coyne, J. D., Telford, N., and Varley, J. M. Identification of a novel fusion gene involving hTAFII68 and CHN from a t(9;17)(q22;q11.2) translocation in an extraskeletal myxoid chondrosarcoma. Oncogene, *18:* 7599–7601, 1999.
32. Sjogren, H., Meis-Kindblom, J., Kindblom, L. G., Aman, P., and Stenman, G. Fusion of the EWS-related gene TAF2N to TEC in extraskeletal myxoid chondrosarcoma. Cancer Res., *59:* 5064–5067, 1999.
33. Shimizu, K., Ichikawa, H., Tojo, A., Kaneko, Y., Maseki, N., Hayashi, Y., Ohira, M., Asano, S., and Ohki, M. An ets-related gene, ERG, is rearranged in human myeloid leukemia with t(16;21) chromosomal translocation. Proc. Natl. Acad. Sci. USA, *90:* 10280–10284, 1993.
34. Panagopoulos, I., Aman, P., Fioretos, T., Hoglund, M., Johansson, B., Mandahl, N., Heim, S., Behrendtz, M., and Mitelman, F. Fusion of the FUS gene with ERG in acute myeloid leukemia with t(16;21)(p11;q22). Genes Chromosomes Cancer, *11:* 256–262, 1994.
35. Ichikawa, H., Shimizu, K., Hayashi, Y., and Ohki, M. An RNA-binding protein gene, TLS/FUS, is fused to ERG in human myeloid leukemia with t(16;21) chromosomal translocation. Cancer Res., *54:* 2865–2868, 1994.

36. Martini, A., La-Starza, R., Janssen, H., Bilhou-Nabera, C., Corveleyn, A., Somers, R., Aventin, A., Foa, R., Hagemeijer, A., Mecucci, C., and Marynen, P. Recurrent rearrangement of the Ewing's sarcoma gene, EWSR1, or its homologue, TAF15, with the transcription factor CIZ/NMP4 in acute leukemia. Cancer Res., *62:* 5408–5412, 2002.
37. Giard, D. J., Aaronson, S. A., Todaro, G. J., Arnstein, P., Kersey, J. H., Dosik, H., and Parks, W. P. *In vitro* cultivation of human tumors: establishment of cell lines derived from a series of solid tumors. J. Natl. Cancer Inst., *51:* 1417–1423, 1973.
38. Gosden, C. M., Davidson, C., and Robertson, M. Lymphocyte culture. *In:* D. E. Rooney and B. H. Czepulkowski (eds.), Human Cytogenetics: A Practical Approach, Vol. 1, Constitutional Analysis, pp. 31–54. Oxford: Oxford University Press, 1992.
39. Roberts, I., Wienberg, J., Nacheva, E., Grace, C., Griffin, D., and Coleman, N. Novel method for the production of multiple colour chromosome paints for use in karyotyping by fluorescence *in situ* hybridisation. Genes Chromosomes Cancer, *25:* 241–250, 1999.
40. Shing, D. C., Morley-Jacob, C. A., Roberts, I., Nacheva, E., and Coleman, N. Ewing's tumour: Novel recurrent chromosomal abnormalities demonstrated by molecular cytogenetic analysis of seven cell lines and one primary culture. Cytogenet. Genome Res., *97:* 20–27, 2002.
41. Kallioniemi, A., Kallioniemi, O. P., Sudar, D., Rutovitz, D., Gray, J. W., Waldman, F., and Pinkel, D. Comparative genomic hybridization for molecular cytogenetic analysis of solid tumors. Science (Wash. DC), *258:* 818–821, 1992.
42. Kumar, S., Pack, S., Kumar, D., Walker, R., Quezado, M., Zhuang, Z., Meltzer, P., and Tsokos, M. Detection of EWS-FLI-1 fusion in Ewing's sarcoma/peripheral primitive neuroectodermal tumor by fluorescence *in situ* hybridization using formalin-fixed paraffin-embedded tissue. Hum. Pathol., *30:* 324–330, 1999.
43. Delattre, O., Zucman, J., Melot, T., Garau, X. S., Zucker, J. M., Lenoir, G. M., Ambros, P. F., Sheer, D., Turc-Carel, C., and Triche, T. J. The Ewing family of tumors: a subgroup of small-round-cell tumors defined by specific chimeric transcripts. N. Engl. J. Med., *331:* 294–299, 1994.
44. Kong, X. T., Ida, K., Ichikawa, H., Shimizu, K., Ohki, M., Maseki, N., Kaneko, Y., Sako, M., Kobayashi, Y., Tojou, A., Miura, I., Kakuda, H., Funabiki, T., Horibe, K., Hamaguchi, H., Akiyama, Y., Bessho, F., Yanagisawa, M., and Hayashi, Y. Consistent detection of TLS/FUS-ERG chimeric transcripts in acute myeloid leukemia with t(16;21)(p11;q22) and identification of a novel transcript. Blood, *90:* 1192–1199, 1997.
45. Panagopoulos, I., Lassen, C., Isaksson, M., Mitelman, F., Mandahl, N., and Aman, P. Characteristic sequence motifs at the breakpoints of the hybrid genes FUS/CHOP, EWS/CHOP and FUS/ERG in myxoid liposarcoma and acute myeloid leukemia. Oncogene, *15:* 1357–1362, 1997.
46. Ichikawa, H., Shimizu, K., Katsu, R., and Ohki, M. Dual transforming activities of the FUS (TLS)-ERG leukemia fusion protein conferred by two N-terminal domains of FUS (TLS). Mol. Cell. Biol., *19:* 7639–7650, 1999.
47. Knezevich, S. R., McFadden, D. E., Tao, W., Lim, J. F., and Sorensen, P. H. A novel ETV6-NTRK3 gene fusion in congenital fibrosarcoma. Nat. Genet., *18:* 184–187, 1998.
48. Eguchi, M., Eguchi-Ishimae, M., Tojo, A., Morishita, K., Suzuki, K., Sato, Y., Kudoh, S., Tanaka, K., Setoyama, M., Nagamura, F., Asano, S., and Kamada, N. Fusion of ETV6 to neurotrophin-3 receptor TRKC in acute myeloid leukemia with t(12;15)(p13;q25). Blood, *93:* 1355–1363, 1999.
49. Tognon, C., Knezevich, S. R., Huntsman, D., Roskelley, C. D., Melnyk, N., Mathers, J. A., Becker, L., Carneiro, F., MacPherson, N., Horsman, D., Poremba, C., and Sorensen, P. H. Expression of the ETV6-NTRK3 gene fusion as a primary event in human secretory breast carcinoma. Cancer Cell, *2:* 367–376, 2002.
50. Lawrence, B., Perez-Atayde, A., Hibbard, M. K., Rubin, B. P., Dal Cin, P., Pinkus, J. L., Pinkus, G. S., Xiao, S., Yi, E. S., Fletcher, C. D., and Fletcher, J. A. TPM3-ALK and TPM4-ALK oncogenes in inflammatory myofibroblastic tumors. Am. J. Pathol., *157:* 377–384, 2000.
51. Siebert, R., Gesk, S., Harder, L., Steinemann, D., Grote, W., Schlegelberger, B., Tiemann, M., Wlodarska, I., and Schemmel, V. Complex variant translocation t(1;2) with TPM3-ALK fusion due to cryptic ALK gene rearrangement in anaplastic large-cell lymphoma. Blood, *94:* 3614–3617, 1999.
52. Lamant, L., Dastugue, N., Pulford, K., Delsol, G., and Mariame, B. A new fusion gene TPM3-ALK in anaplastic large cell lymphoma created by a (1;2)(q25;p23) translocation. Blood, *93:* 3088–3095, 1999.
53. Ladanyi, M. Aberrant ALK tyrosine kinase signaling. Different cellular lineages, common oncogenic mechanisms. Am. J. Pathol., *157:* 341–345, 2000.